A CONTOUR MATCHING APPROACH FOR ACCURATE NOAA-AVHRR IMAGE NAVIGATION

Francisco Eugenio[1], Ferran Marqués[2], Eduardo Suárez[1], and Eduardo Rovaris[1]

[1]Signal and Communications Department. University of Las Palmas of G.C.
[2]Signal Theory and Communications Department. Polytechnic University of Catalonia.
Campus Universitario de Tafira. Edificio de Electrónica y Telecomunicación.
35017 Las Palmas de G.C., Spain
Tel: +34 928 452979; Fax: +34 928 451243
E-mail: feugenio@dsc.ulpgc.es

ABSTRACT

Although different methods for NOAA AVHRR image navigation have already been established, the multitemporal and multi-satellite character of most studies requires automatic and accurate methods for navigation of satellite images. In the proposed method, a simple Kepplerian orbital model for the NOAA satellites is considered as reference model, and mean orbital elements are given as input to the model from ephemeris data. In order to correct the errors caused by these simplifications, errors resulting from inaccuracies in the positioning of the satellite and failures in the satellite internal clock, an automatic global contour matching approach has been adopted. First, the sensed image is preprocessed to obtain a gradient energy map of the reliable areas (sea-land contours) using a cloud detection algorithm and a morphological gradient operator. An initial estimation of the reliable contour positions is automatically obtained. The final positions of the contours are obtained by means of an iterative local minimization procedure that allows a contour to converge on an area of high image energy (edge). Global transformation parameters are estimated based on the initial and final positions of all reliable contour points. Finally, the performance of this approach is assessed using NOAA 14 AVHRR images from different geographic areas.

1 INTRODUCTION

The sea surface temperature (SST) is an important geophysical parameter, essential for quantitative studies of the Earth atmosphere and oceans. The SST imagery remotely sensed by the Advanced Very High Resolution Radiometer (AVHRR) aboard the NOAA satellite series has been conveniently used in various fields; for example, oceanography, meteorology, fishery, etc.

The characteristic of the satellite scanning, which covers, approximately, a 2800 Km wide swath, the spacecraft's speed, altitude and attitude and the Earth's curvature and rotation, produce significant distortions in the images. The exact geographic location of any pixel is necessary for a comparison among images, particularly in sequential image analysis or multi-satellite image studies. Therefore, it is necessary for image referencing to identify the geographic co-ordinates corresponding to an image pixel (direct referencing) or to locate a pixel corresponding to given geographic co-ordinates (inverse referencing). It is this inverse referencing that has become the default definition of AVHRR image navigation today.

A good overview of existing methods of AVHRR image navigation is given by Emery et al [5] and Krasnopolsky et al [10]. In these references, several models of varying complexity can be found, ranging from the locally circular orbit approach (Ho and Asem [7], Bachmann and Bendix [2]), to complex elliptical orbits in which perturbations caused by the Earth's oblateness, the gravitation effects of the Sun and Moon, etc..., are taken into account (Brunel and Marsouin [3]).

The accuracy obtained from the application of these models is variable. Failures in the satellite's internal clock, lack of knowledge concerning the attitude angles and inaccuracies in Kepplerian orbital elements give rise to the fact that even the most complex models do not offer the desired accuracy of errors of less than one pixel. To achieve this accuracy, the use of Ground Control References Points (GCPs) has been proposed (Moreno et al [11], Rosborough et al [13] and Illera et al [8]). A procedure for automatically navigating AVHRR images using both Argos and TBUS orbital elements was developed by Brunel and Marsouin [3]. The automation in the determination of GCP's, by means of correlation techniques in slave and master images, was described by Cracknell and Paithoonwattanakij [4].

Our objective is to derive a fully automatic and operational procedure for the navigation of NOAA-AVHRR images with high accuracy and without GCP's, based on the simultaneous use of an orbital model and a contour matching approach. The orbital model assumes a circular orbit [2], [7], [8], using nominal Keplerian orbital elements and nominal nodal parameters obtained from the NOAA weekly archive of the Equator crossing. To correct the errors caused by these simplifications, nonzero value for the spacecraft's roll, pitch and yaw and failures in the satellite internal clock, an automatic contour matching approach has been adopted. It allows the detection and extraction of land contours (islands and continent, in our case) having cloud occlusion, in both day and night images.

In the next sections, the theoretical bases and a practical application of the procedure are presented.

2 GLOBAL CONTOUR MATCHING ALGORITHM

The contours overlay that is obtained after processing the geographical data available at the CIA World Data Base I (Anderson [1]) is used as the reference contours in the minimization process (reference image). The automatic global contour matching procedure is summarized by the following steps, which are described in the subsequent sections:

1) Preprocessing: Application of a cloud detection algorithm and a morphological gradient operator to determine the reliable areas of the sensed image and use of an edge estimation to obtain a gradient energy map.
2) Contour position initialization: The Euclidean distance between the reference image and the validated objects in the sensed image is minimized.
3) Local minimization: Contours in the reference image are locally minimized on the gradient energy map of the sensed image.
4) Global optimization: Conflict resolution to detect true contours and eliminate false alarms. Global parameters are obtained using the true contours and the whole image is re-mapped.

I. PREPROCESSING

A major problem in contour matching between the reference image objects and the contour objects in the sensed image is the presence of clouds (clutter) which would lead to errors and false detection when matching contours. It is highly desirable to remove these irrelevant features before detection and analysis. Once the cloud overlay is obtained by a multi-band threshold method [12], we determine the cloud-sea and the cloud-land contours (useless pixels) applying a morphological gradient. This way, the non-reliable and reliable areas (sea-land contours) to which contours will be allowed to match are obtained.

The contour matching procedure requires an estimation of the contour positions in the sensed image. We determine the gradient energy map normalized by means of,

$$[1]E_{edge} = -G_{\sigma} * |\overline{\nabla I(x,y)}|^2 \qquad (1)$$

where G_σ is a two-dimensional Gaussian function with standard deviation σ, used to facilitate the convergence of the contours to the image gradients.

II. CONTOUR POSITION INITIALIZATION

The matching contour model approach is an iterative energy minimization process, which starts from an initial estimate. If an initial boundary is placed too far from the solution boundary, the contour might converge erroneously to an undesirable position. Usually, the initialization issue is application specific, requiring either prior knowledge or user iteration. We propose an automatic initialization process for the satellite images, based on the minimization of the Euclidean distance between the centers of gravity of closed boundaries in the reference image and the corresponding objects detected in the sensed image. The center of gravity of an object of a binary image *f(i,j)* can be given by using object moments (Jain [9]),

$$x = \frac{\sum_i \sum_j j \cdot f(i,j)}{m_{00}} \qquad y = \frac{\sum_i \sum_j i \cdot f(i,j)}{m_{00}} \qquad (2)$$

where m_{00} represents the binary object area (zero-order moment). To detect and extract the objects, the sensed image is segmented using a non-spatial iterative threshold selection technique [9], and the corresponding land objects are labeled by a sequential algorithm.

III. LOCAL MINIMIZATION

The minimization algorithm allows a contour to converge on an area of high image energy, in this case edges. Given a set of m contours of n_i points corresponding, for example, to an island, the algorithm allows movements in a neighborhood of size w at each iteration.

Let $\mathbf{V}_i^{(k)} = \{v_{i\,j}^{(k)} \mid j=1,2,...,n_i\}$ be the i-th contour after the *k-th* iteration. Its total energy is,

$$E_{contour_i}^{(k)} = E_{contour}(\mathbf{V}_i^{(k)}) = \sum_{j=1}^{n_i} e(v_{i\,j}^{(k)}) \qquad (3)$$

where e(·) is the energy of the *j-th* point of the contour.

Suppose a search window W centered at the current position is generated in which every position is a candidate point for updating. The algorithm moves $\mathbf{V}_i^{(k)}$ to a new location $\mathbf{V}_i^{(k+1)}$ according to the following updating rule,

$$\mathbf{V}_i^{(k+1)} = arg\,min\, E_{contour}(\mathbf{V}_i^{(k)}) \qquad (4)$$

In this respect, the contour matching model transforms the boundary detection process into an optimization problem. After each updating, the contour energy $E_{contour_i}^{(k+1)}$ decreases. At each iteration, we calculate the minimum energy for each contour of the overlay in the image. When $E_{contour}^{(k+1)} = E_{contour}^{(k)}$, the contour has not found a position with less energy and so the process ends.

IV. GLOBAL OPTIMIZATION

The global optimization is based on the data obtained in the previous step and we consider a three-step procedure. First, a post-processing stage to resolve misdetection and to eliminate false detection; second a least-square fitting procedure; and a final re-navigation of the whole image to fit to the selected map projection using correction functions.

There are two types of errors in the automatic contour matching: 1) Misdetection and 2) False detection. Misdetection is primarily due to the total occlusion of the contour corresponding to an island or a continent. False detection is caused by detection and matching of a small part of a coastline that does not correspond with a true

[1] $|\overline{\nabla I}|$ is the gradient intensity normalized to [0,1]

position. Both errors are undesirable in the procedure of global optimization. We have adopted a strategy to first count the number of potential desirable contours points of each island and continent obtained in the pre-processing step. Then, contours not having any points of the desired contour due to total occlusion (misdetection) or having less than 10% of the desired number of points (false detection) are removed.

The global parameters are obtained by performing a bilinear regression from the initial (X_I,Y_I) and final (X_O,Y_O) positions of each of the validated points obtained in the complete minimization process (contour initialization and local minimization). It is often assumed that the relationship between sensed image, obtained from orbital model, and reference image can be expressed by a 2-D affine transform [7] [9], since the systematic errors have previously been compensated by the orbital model. The global transformation follows an affine model that leads to the following correction functions (in vector-matrix form):

$$\begin{bmatrix} X_O \\ Y_O \end{bmatrix} = \begin{pmatrix} A_X \\ A_Y \end{pmatrix} + \begin{pmatrix} B_X & C_X \\ B_Y & C_Y \end{pmatrix} \cdot \begin{bmatrix} X_I \\ Y_I \end{bmatrix} \qquad (5)$$

This allows generating transformations with respect to rotation, scaling and translation. Finally, the image is then re-navigated using the correction function. This procedure is performed globally, so the islands (or portions of them), that could not be detected in the contour matching process, are now detected. That is, given the global nature of the bilinear regression, it estimates the position of all land contours, even those covered by clouds.

3 RESULTS

In order to experiment with different types of satellite images, we have developed a user-interface for contour matching. The interface has been designed to be user friendly, easy to learn and to make easier the work of future users. The interface allows a user selecting the type of edge detector, normalization functions, starting points and monitoring contour positions. Moreover it is possible to see the cloudy areas, gradient map and useful and useless pixels of the image. In addition to its value as a research tool, the user-interface has proven very useful for accurate tracking of contour features.

The proposed algorithm has been tested in a large set of satellites images, showing Table 1 the results obtained for a subset of five NOAA 14-AVHRR images representing ascending and descending paths as well as different sub-satellites position. In Table 1, the captured data is shown jointly with the orbit number and the resulting of the fitting of equation (5). Errors less than 0.64 row/col are obtained.

Table 1. Results of NOAA-AVHRR image referencing for five test cases.

Image Orbit number	Trajectory Offset Nadir	Results of the fitting function (5)	A	B	C	RMS
9 January 1997 10457	S/N 6.55º	**X**	-1.087	1.008	-0.004	0.51
		Y	2.398	-0.002	0.996	0.48
18 January 1998 15727	S/N -9.63º	**X**	2.605	0.996	-0.009	0.43
		Y	12.29	0.001	1.004	0.63
6 June 1998 17688	N/S 13.35º	**X**	4.887	1.007	-0.004	0.61
		Y	8.398	-0.002	0.998	0.74
3 July 1999 23227	S/N -35.27º	**X**	5.587	0.995	-0.001	0.43
		Y	15.29	0.001	1.003	0.48
1 January 2000 25788	N/S 22.48º	**X**	-4.546	1.001	0.002	0.63
		Y	-6.473	0.001	1.002	0.84
	R.M.S. Error Average				**X**	0.52
					Y	0.63

An example of a NOAA 14-AVHRR geo-referenced image is shown in Figure 1. The data represent Sea Surface Temperature (SST) from an ascending pass taken on July 3, 1999 at 15:54:48 GMT. The image is 411*902 pixels and it depicts Canary Islands and NW Coast of Africa. The sequence given in Fig.1 shows intermediate and final results of the algorithm. Fig.1(a) shows the classification of the pixels into useful and useless ones for the contour matching approach and the offset of the sensed image from the reference image as the result of the geo-referencing errors in the orbital model. In Fig.1(b), the correspondence between the overlay and the image shows that the registration obtained by our algorithm is accurate to within a pixel, for the cloudless zones as well as for the zones having occlusions.

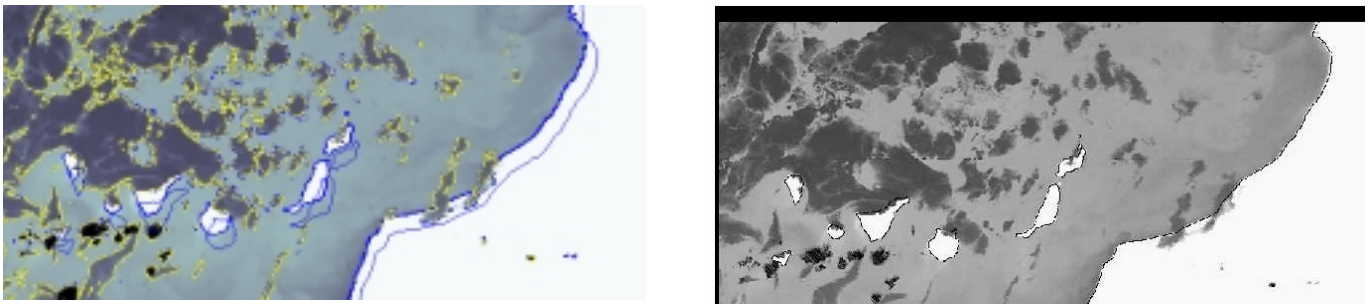

Figure 1. NOAA 14 -AVHRR image of 3 July 1999 georeferenced into the UTM map projection. a) Classification of the useful (blue contour) and useless (yellow contour) pixels and the offset of the sensed image from the reference image, and b) results of the contour matching approach showing the correspondence between the reference and sensed images.

Figure 2 and 3 show the results achieved by the proposed method in images of the Canary Islands area and Strait of Gibraltar area, respectively. Note that both examples contain portions with partial and total occlusions. The results present accurate estimations of the location of all regions (even the non-visible ones).

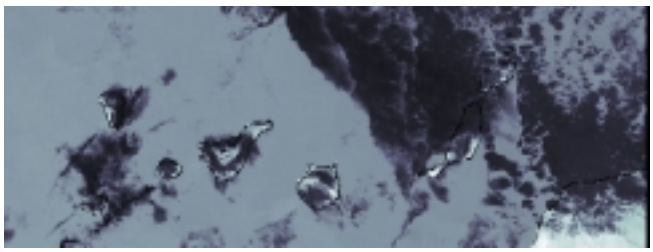

Figure 2. Results of contour matching approach applied to NOAA 14-AVHRR image (Canary Islands area) of 9 January 1997.

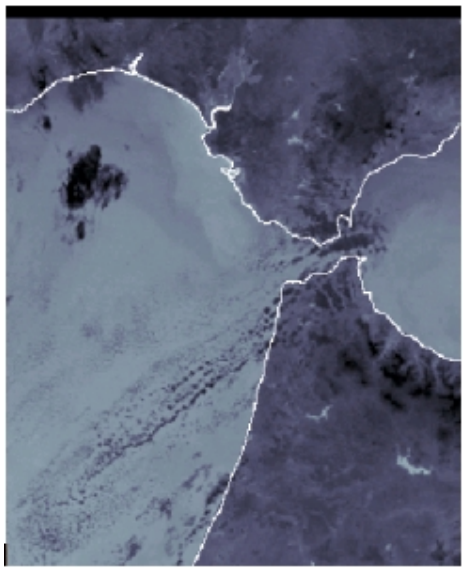

Figure 3. Results of contour matching approach applied to NOAA14 -AVHRR image(Strait of Gibraltar area)of 6 June 1998.

4 CONCLUSION

The algorithm proposed is automatic, robust, and of significant value in an operational context. The performance of the algorithm has been demonstrated by navigation of NOAA AVHRR images taken in different years, proving to be capable of geo-referencing satellite images within one pixel error. We conclude that this type of algorithm is adequate for automatic navigating satellite images, even when using a simple orbital model. Although the method has been developed to be applied to AVHRR data, it is general, and it can be applied to any sensor similar to AVHRR on board of a satellite similar to the NOAA series.

The favorable results from this study have spawned a follow-up project that consists of the simultaneous optimization of the entire set of image contours by means of the energy minimization in the field of the global transformation parameters [6].

Acknowledgments

We wish to express our gratitude to the Educational Council of the Canary Islands Government (Contract PI 1998/066), Canaries Technological Institute (Telesat Project) and CICYT-Commission of the European Communities (Project 1FD97-1167). We would like to express our special gratitude to Mr. Javier Marcello for his help and support.

References

[1] D.E. Anderson et al, "World Data Bank II: Content, Structure and Applications, Washington D.C.: Office of Geographic and Cartographic Research, Central Intelligence Agency, 1973.

[2] M. Bachmann and C. Bendix, , "An improved algorithm for NOAA-AVHRR image referencing," Int. Journal Remote Sensing, vol. 13, pp. 3205-3215, 1992.

[3] P. Brunel and A. Marsouin, "An operational method using Argos orbital elements for navigation of AVHRR imagery," Int. Journal of Remote Sensing, vol. 8, pp. 569-578, 1987.

[4] A.P. Cracknell and K. Paithoonwattanakij, "Pixel and sub-pixel accuracy in geometrical correction of AVHRR imagery," Int. Journal of Remote Sensing, vol. 10, pp. 661-667, 1989.

[5] W.J. Emery et al., "AVHRR image navigation: Summary and review," Photogrammetric Engin. Remote Sensing, vol. 55, pp. 1175-1183, 1989.

[6] F. Eugenio and F. Marqués, " Accurate and Automatic NOAA-AVHRR image navigation using a global contour matching approach," in press, Proc. Int. Geosciencie and Remote Sensing Symp., IGARSS'2000, Hawaii, U.S., July 24-28.

[7] D. Ho and A. Asem, "NOAA AVHRR image referencing," Int. Journal of Remote Sensing, vol. 7, pp. 895-904, 1986.

[8] P. Illera et al., "A navigation algorithm for satellite images," Int. Journal of Remote Sensing, vol. 17, pp. 577-588, 1996.

[9] Anil K. Jain, "Fundamentals of Digital Image Processing," Prentice Hall International, 1989.

[10] V.M. Krasnopolsky and D. Breaker, "The problem of AVHRR image navigation revisited," Int. Journal Remote Sensing, vol. 15, pp. 979-1008, 1994.

[11] J.F. Moreno and F. Meliá, "A method for accurate geometric correction of NOAA AVHRR HRPT data," IEEE Transaction on Geosciencie and Remote Sensing, vol. 31, pp. 204-226, January 1993.

[12] P. W. Saunders and K.T. Kriebel, "An improved method for detecting clear sky radiances from AVHRR data," Int. Journal of Remote Sensing, vol. 9, pp. 123-150, 1988.

[13] G.W. Rosborough et al., "Precise AVHRR image navigation," IEEE Transaction on Geosciencie and Remote Sensing, vol. 32, pp. 644-657, May 1994.